

University of Nebraska - Lincoln

DigitalCommons@University of Nebraska - Lincoln

Anthony F. Starace Publications

Research Papers in Physics and Astronomy

April 1977

Measurement of the Xenon $\sigma_{3/2}:\sigma_{1/2}$ Branching Ratio within the Xe 5s5p⁶6p(¹P₁) Resonance

Peter C. Kemeny

University of Nebraska - Lincoln, peter.kemeny@KemenyConsulting.com.au

James A. R. Samson

University of Nebraska - Lincoln

Anthony F. Starace

University of Nebraska-Lincoln, astarace1@unl.edu

Follow this and additional works at: <https://digitalcommons.unl.edu/physicsstarace>

 Part of the [Physics Commons](#)

Kemeny, Peter C.; Samson, James A. R.; and Starace, Anthony F., "Measurement of the Xenon $\sigma_{3/2}:\sigma_{1/2}$ Branching Ratio within the Xe 5s5p⁶6p(¹P₁) Resonance" (1977). *Anthony F. Starace Publications*. 159.
<https://digitalcommons.unl.edu/physicsstarace/159>

This Article is brought to you for free and open access by the Research Papers in Physics and Astronomy at DigitalCommons@University of Nebraska - Lincoln. It has been accepted for inclusion in Anthony F. Starace Publications by an authorized administrator of DigitalCommons@University of Nebraska - Lincoln.

Submitted February 14, 1977

LETTER TO THE EDITOR

Measurement of the Xenon $\sigma_{3/2} : \sigma_{1/2}$ Branching Ratio within the Xe 5s5p⁶6p(¹P₁) Resonance

Peter C. Kemeny, James A. R. Samson, and Anthony F. Starace

Behlen Laboratory of Physics, University of Nebraska–Lincoln
Lincoln, Nebraska 68588, USA

Abstract

Photoionization of the 5p⁶ shell in xenon leaves the ion in either the 5p⁵(²P_{3/2}) or np⁵(²P_{1/2}) state. Measurements of the $\sigma_{3/2} : \sigma_{1/2}$ branching ratio are reported within the Xe 5s5p⁶6p(¹P₁) resonance and fitted to a new theoretical expression. The maximum value of the ratio as determined by a two-parameter fit of theory to experiment is 8.8 ± 0.5 within the resonance, almost six times the nearly constant value of 1.55 found outside any resonance.

Photoionization of the outer np⁶(¹S₀) subshell of the rare gases leaves the ion in either the np⁵(²P_{3/2}) or np⁵(²P_{1/2}) state. The ratio of the cross sections for these two alternative reactions has been found experimentally to be remarkably constant and non-statistical over a photon energy range of approximately 25 eV above the np⁶(¹S₀) ionization threshold (Samson and Cairns 1968, Samson *et al.* 1975). These earlier measurements, the analysis of which required some estimated values for the asymmetry parameter β , indicated that a large change in the ratio *may* occur within autoionizing resonances, presumably due to strong electron correlations, but since only discrete emission lines were available at that time, it was impossible to study the ratio systematically across a resonance. This letter reports the first measurement of this ratio as a function of wavelength within a resonance; the experimental data presented is unaffected by any variations in the photoelectron angular distribution. The particular resonance chosen is the xenon 5s5p⁶6p(¹P₁) autoionizing level at 20.95 eV. Whereas the off-resonance ratio $\sigma_{3/2} : \sigma_{1/2}$ has been found to be nearly constant at 1.55 ± 0.08 (Samson and Cairns 1968, Samson *et al.* 1975), well *below* the statistical ratio of 2.0, we find that within the resonance this ratio increases sharply from its off-resonance value to values greater than three. The experimental data have been fitted to a two-parameter theoretical formula of Starace (1977), and related to the Fano profile parameters determined by Ederer (1971, 1976) for this resonance. The present experimental data demonstrate the strength of electron correlation within small energy regions, as found previously for the photoelectron asymmetry parameter within a resonance (Samson and Gardner 1973, Dill 1973). Furthermore the present branching-ratio data, together with the line-profile data, provide experimental information on the theoretical matrix elements needed to characterize the autoionizing resonance Xe 5s5p⁶6p(¹P₁) completely.

The xenon $\sigma_{3/2}:\sigma_{1/2}$ branching ratio within the $5s5p^6p(^1P_1)$ autoionizing resonance was measured as a function of wavelength by the technique of photoelectron spectroscopy. Both the electron energy analyzer and the method used to determine the branching ratio have been described in detail previously (Samson *et al.* 1975, Gardner and Samson 1973, 1975). For orientation, a portion of the photoabsorption of xenon in the region of the resonance of interest, labeled 3, is shown in Figure 1. The energy scale is centered on the resonance energy, $E_{\text{res}} = 20.951$ eV (591.77 Å), and refers to the reduced energy variable $\epsilon = (\hbar\omega - E_{\text{res}})/\frac{1}{2}\Gamma$ where $\hbar\omega$ is the photon energy and $\Gamma = (31.2 \pm 0.8)$ meV is the resonance width given by Ederer (1971, 1976). Synchrotron radiation from the electron storage ring Tantalus 1 at Stoughton, Wisconsin, in conjunction with a horizontally dispersing normal-incidence monochromator, provided a continuously tunable light source over the wavelength region of interest.

The wavelength calibration of the monochromator was performed by back-filling the electron energy analyzer chamber with about 10 μ of xenon and then observing the attenuation of the photon beam from the monochromator as a function of wavelength using a photocathode appropriately positioned within the analyzer chamber. Peaks in the photocurrent corresponding to resonances 3 and 4 in Figure 1 were observed, yielding a wavelength calibration accurate to about 0.1 Å. The resolution of the monochromator was set at 0.3 Å (FWHM) at 584.3 Å, based on the observed width of the He I resonance line, which has a natural width of only approximately 5 meV (Samson 1969). Higher resolution could be obtained from the monochromator, but the attendant decrease in intensity would have made the measurements described here impracticable. A monochromator resolution of 0.3 Å yields accurately measured branching ratios *away* from the center and wings of the resonance. Correction would be required for branching ratios measured within 0.2 Å of the absorption minimum in the resonance. However, it was not possible to obtain accurate ratios in this region because of the very weak

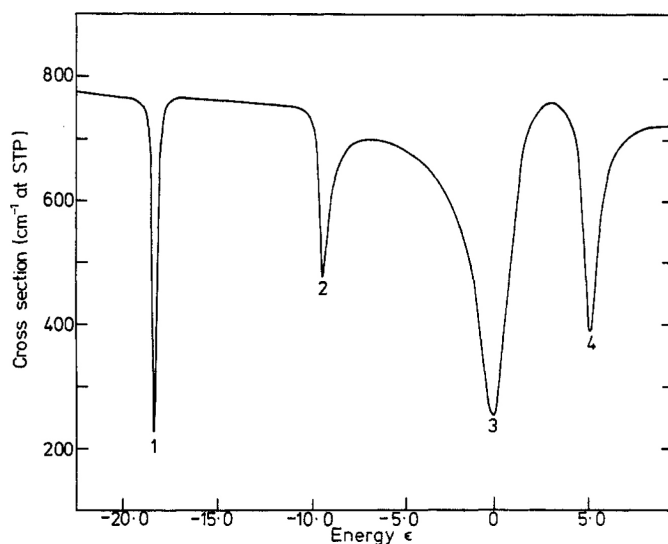


Figure 1. Photoabsorption cross section of xenon taken from figure 2 of Ederer (1971) plotted against the reduced photon energy ϵ defined in the text. The xenon $5s5p^6p(^1P_1)$ resonance, indicated by code number 3, occurs at 20.951 eV (591.77 Å). This figure incorporates corrections to figure 2 of Ederer (1971) necessitated by Ederer (1976).

signals generated. Although the $\sigma_{3/2}$ signal was observed at the minimum, the $\sigma_{1/2}$ signal could not be seen above the background noise.

The photon flux from the exit slit of the monochromator at a wavelength of 600 Å was determined to be about $4 \times 10^8 \text{ s}^{-1}$ with a beam current of 100 mA circulating in the storage ring. To maintain a high pressure differential between the electron energy analyzer chamber and the monochromator, a 1000 Å aluminum window was used, allowing a net photon flux of $8 \times 10^7 \text{ s}^{-1}$ to the analyzer. Electron energy analysis and detection was performed with a turbomolecular pumped cylindrical mirror analyzer (CMA) (Samson *et al.* 1975, Gardner and Samson 1973, 1975) in conjunction with an ND 2400 multichannel analyzer. The xenon $\sigma_{3/2}:\sigma_{1/2}$ branching ratio was taken to be the ratio of the corresponding integrated peak areas in the photoelectron spectrum, corrected for the electron energy analyzer transmission efficiency (Gardner and Samson 1975), which varies with photoelectron kinetic energy. The pressure of the xenon gas was maintained at a constant value for all data points.

The photon beam from the monochromator was collinear with the axis of the CMA, and collimating slits in the reaction region of the energy analyzer accepted a cone of photoelectrons making an angle of 54.7° with the photon beam. This collection geometry ensures that the measured signal is proportional to the cross sections $\sigma_{3/2}$ and $\sigma_{1/2}$, and not to the differential cross sections $d\sigma_{3/2}/d\Omega$ and $d\sigma_{1/2}/d\Omega$, as may be seen from equation (7) of Samson and Starace (1975).

Our measured $\sigma_{3/2}:\sigma_{1/2}$ branching ratios within the Xe 5s5p⁶p(¹P₁) autoionizing resonance are shown as a function of photon energy (given in units of ϵ) in Figure 2, together with a theoretical fit to this data, described below. Each experimental point represents approximately 9 h of data acquisition time. The error bars indicate the statistical accuracy of the measured branching ratios.

The full curve in Figure 2 represents a fit to the experimentally measured branching ratio of the following theoretical formula (derived by Starace (1977)) for the behavior of $\sigma_{3/2}:\sigma_{1/2}$ as a function of ϵ in the neighborhood of an isolated resonance:

$$\frac{\sigma_{3/2}}{\sigma_{1/2}} = \left(\frac{\sigma_{3/2}}{\sigma_{1/2}} \right)_0 \frac{\{\epsilon^2 + 2\epsilon(q \operatorname{Re} \langle \alpha \rangle_{3/2} - \operatorname{Im} \langle \alpha \rangle_{3/2}) + [1 - 2q \operatorname{Im} \langle \alpha \rangle_{3/2} - 2 \operatorname{Re} \langle \alpha \rangle_{3/2} + (q^2 + 1) \langle |\alpha|^2 \rangle_{3/2}]\}}{\{\epsilon^2 + 2\epsilon(q \operatorname{Re} \langle \alpha \rangle_{1/2} - \operatorname{Im} \langle \alpha \rangle_{1/2}) + [1 - 2q \operatorname{Im} \langle \alpha \rangle_{1/2} - 2 \operatorname{Re} \langle \alpha \rangle_{1/2} + (q^2 + 1) \langle |\alpha|^2 \rangle_{1/2}]\}}. \quad (1)$$

Here q is the Fano profile parameter (Fano 1961) associated with the resonance, ϵ is the reduced energy variable described above, $(\sigma_{3/2}/\sigma_{1/2})_0$ is the value of the branching ratio outside the resonance, and the parameters $\langle \alpha \rangle_{3/2}$, $\langle |\alpha|^2 \rangle_{3/2}$, $\langle \alpha \rangle_{1/2}$, $\langle |\alpha|^2 \rangle_{1/2}$ are weighted averages of the quantities $\alpha(\mu E_{\text{res}})$ and $|\alpha(\mu E_{\text{res}})|^2$, where

$$\alpha(\mu E_{\text{res}}) \equiv \frac{\langle \phi | \sum_i > j 1/r_{ij} | \mu E_{\text{res}} \rangle}{\langle g | \sum_i r_i | \mu E_{\text{res}} \rangle} \left(\frac{2\pi K}{\Gamma} \right). \quad (2)$$

In equation (2), the Coulomb interaction matrix element is between the resonance state ϕ and the observable photoelectron channel μ having the same total energy E_{res} as the state ϕ . The electric dipole matrix element is between the ground state g of the atom and the photoelectron channel μ having total energy E_{res} . Note that these matrix elements are complex since they involve a summation over the phaseshifts of the system's eigenchannels (Starace 1977). The remaining

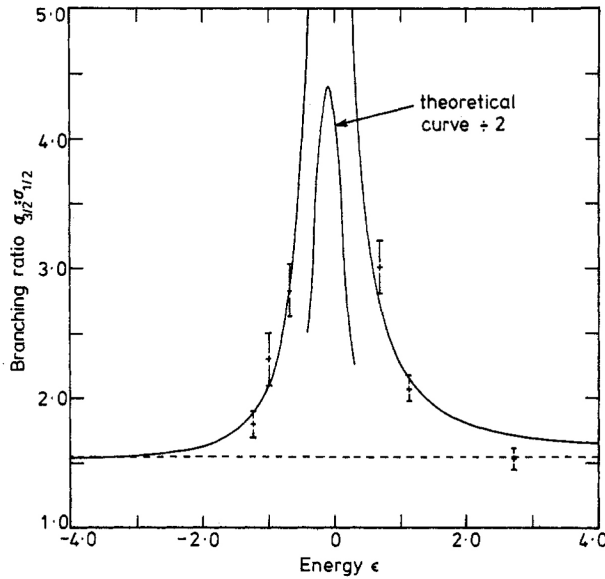


Figure 2. Photoelectron branching ratio $\sigma_{3/2}:\sigma_{1/2}$ for xenon in the neighborhood of the xenon $5s5p^6p(^1P_1)$ autoionizing resonance. The reduced photon energy ϵ is the same as in Figure 1. The error bars about each of the experimentally measured points indicate their statistical uncertainty. The full curve represents the theoretical curve obtained from Equation (8a) using the fitted parameters C_1 and C_2 defined in Equation 8. The broken line is the measured off-resonance value of the branching ratio, $(\sigma_{3/2}/\sigma_{1/2})_0 = 1.55$ as given by Samson *et al.* (1975).

factors K and Γ (the resonance width) relate to the resonance ϕ as a whole and not to any particular photoelectron channel μ . They are given by

$$\Gamma \equiv 2\pi \sum_{\mu} \left| \left\langle \phi \left| \sum_{i>j} 1/r_{ij} \right| \mu E_{\text{res}} \right\rangle \right|^2 \quad (3)$$

$$K \equiv \sum_{\mu} \left\langle g \left| \sum_i r_i \right| \mu E_{\text{res}} \right\rangle \left\langle \mu E_{\text{res}} \left| \sum_{i>j} 1/r_{ij} \right| \phi \right\rangle \quad (4)$$

where the summations extend over all observable photoelectron channels μ . The averages of $a(\mu E_{\text{res}})$ are taken over the set of photoelectron channels μ belonging to either the $^2P_{3/2}$ or $^2P_{1/2}$ state of the ion and are weighted by the squares of the electric dipole transition matrix elements, *e.g.*

$$\langle \alpha \rangle_{3/2} \equiv \frac{\sum_{\mu \in ^2P_{3/2}} |\langle g | \sum_i r_i | \mu E_{\text{res}} \rangle|^2 \alpha(\mu E_{\text{res}})}{\sum_{\mu \in ^2P_{3/2}} |\langle g | \sum_i r_i | \mu E_{\text{res}} \rangle|^2}. \quad (5)$$

Similarly, $\langle |a|^2 \rangle_{3/2}$ is the weighted average of $|a(\mu E_{\text{res}})|^2$.

The α parameters are not independent. They may be related to each other as follows (Starace 1977):

$$\left(\frac{\sigma_{3/2}}{\sigma_{1/2}} \right)_0 \langle |a|^2 \rangle_{3/2} + \langle |a|^2 \rangle_{1/2} = \rho^2 \left[1 + \left(\frac{\sigma_{3/2}}{\sigma_{1/2}} \right)_0 \right] \quad (6a)$$

$$\left(\frac{\sigma_{3/2}}{\sigma_{1/2}} \right)_0 \text{Re} \langle \alpha \rangle_{3/2} + \text{Re} \langle \alpha \rangle_{1/2} = \rho^2 \left[1 + \left(\frac{\sigma_{3/2}}{\sigma_{1/2}} \right)_0 \right] \quad (6b)$$

$$\left(\frac{\sigma_{3/2}}{\sigma_{1/2}}\right)_0 \text{Im} \langle \alpha \rangle_{3/2} + \text{Im} \langle \alpha \rangle_{1/2} = 0. \quad (6c)$$

In equation (6), ρ^2 is the correlation index (Fano and Cooper 1965), which is another of the Fano profile parameters. Equation (6) may be used to solve for $\langle |\alpha|^2 \rangle_{1/2}$, $\text{Re} \langle \alpha \rangle_{1/2}$, and $\text{Im} \langle \alpha \rangle_{1/2}$ in terms of the three independent parameters $\langle |\alpha|^2 \rangle_{3/2}$, $\text{Re} \langle \alpha \rangle_{3/2}$, and $\text{Im} \langle \alpha \rangle_{3/2}$, whose values can be shown to be restricted by the following bounds (Starace 1977):

$$\rho^2 \left[1 + \left(\frac{\sigma_{3/2}}{\sigma_{1/2}} \right)_0 \right] \geq \langle |\alpha|^2 \rangle_{3/2} \geq (\text{Re} \langle \alpha \rangle_{3/2})^2 + (\text{Im} \langle \alpha \rangle_{3/2})^2. \quad (7)$$

Thus, provided the profile parameters q , Γ , and ρ^2 are known, and – provided the branching ratio outside the resonance $(\sigma_{3/2}/\sigma_{1/2})_0$ is known – one may predict the behavior of the branching ratio in the vicinity of a resonance by calculating *ab initio* values for $\langle |\alpha|^2 \rangle_{3/2}$ and $\langle \alpha \rangle_{3/2}$ and substituting them into Equations (1) and (6).

One cannot, however, obtain $\langle |\alpha|^2 \rangle_{3/2}$, $\text{Re} \langle \alpha \rangle_{3/2}$, and $\text{Im} \langle \alpha \rangle_{3/2}$ by fitting Equation (1) to experimental data since, after substituting Equation (6) into Equation (1), one finds that Equation (1) depends on only two independent linear combinations of the α parameters:

$$\frac{\sigma_{3/2}}{\sigma_{1/2}} = r \left(\frac{\epsilon^2 + 2\epsilon C_1 + (1 + C_2)}{\epsilon^2 + 2\epsilon [q\rho^2(1+r) - rC_1] + [1 + (q^2 - 1)\rho^2(1+r) - rC_2]} \right) \quad (8a)$$

where

$$C_1 \equiv q \text{Re} \langle \alpha \rangle_{3/2} - \text{Im} \langle \alpha \rangle_{3/2} \quad (8b)$$

$$C_2 \equiv (q^2 + 1) \langle |\alpha|^2 \rangle_{3/2} - 2q \text{Im} \langle \alpha \rangle_{3/2} - 2 \text{Re} \langle \alpha \rangle_{3/2} \quad (8c)$$

$$r \equiv \left(\frac{\sigma_{3/2}}{\sigma_{1/2}} \right)_0. \quad (8d)$$

The two linear combinations of coefficients, C_1 and C_2 , were determined by fitting equation (8a) to experimental data using a two-parameter least-squares optimization procedure. The values $q = 0.23 \pm 0.04$ and $\rho^2 = 0.65 \pm 0.03$ used in equation (8a) were obtained from Ederer (1971, 1976); the value $(\sigma_{3/2}/\sigma_{1/2})_0 = 1.55 \pm 0.08$ was obtained from Samson *et al.* (1975). Our fitted values for the two independent parameters are:

$$C_1 = 0.176 \pm 0.005$$

$$C_2 = -0.437 \pm 0.0403.$$

Slight changes in the parameters C_1 and C_2 can cause substantial changes in the theoretical peak value of the branching ratio. With the possible errors in C_1 and C_2 quoted above, the peak value of the fitted branching ratio curve, 8.8, has an uncertainty of ± 0.5 . Note that the errors quoted for C_1 and C_2 are those appropriate for the fit obtained; the errors in the profile parameters and in $(\sigma_{3/2}/\sigma_{1/2})_0$ are not accounted for in the errors given for C_1 and C_2 . Furthermore, the fitting procedure took no account of the experimental uncertainty in the energy positions of the measured cross sections. An upper limit of this uncertainty is approximately 0.1 Å, as mentioned above, which implies a maximum uncertainty in ϵ of about 0.2. As to the applicability of equations (1) and (8a), which hold for an isolated resonance, note that all experimental points in Figure 2, except the one at $\epsilon =$

2.7, lie approximately within a halfwidth (*i.e.* $\frac{1}{2}\Gamma$) of the position of resonance 3 in Figure 1. The point at $\epsilon = 2.7$ in Figure 2 falls midway between resonances 3 and 4 in Figure 1. Hence this experimental point may not be fitted well by any isolated resonance formula such as Equation (1) or Equation (8a).

The experimental data presented here thus represent the first definitive measurement of the behavior of a photoelectron branching ratio within an autoionizing resonance. Within the resonance, the branching ratio is found experimentally to vary considerably, in contrast to its nearly constant behavior outside the resonance region (Samson and Cairns 1968, Samson *et al.* 1975), and this behavior is reproduced closely by the theory which contains just two adjustable parameters. This demonstrates the strength of even weak interactions, such as the spin-orbit interaction, within small energy regions (Fano 1970). In particular, *ab initio* calculations of the α parameters in Equation (1) (and hence of C_1 and C_2) would provide a test of theoretical methods for incorporating spin-orbit and other relativistic interactions into atomic collision computations. Furthermore, measurements of the photoelectron branching ratio within a resonance provide a check of the profile parameters obtained in photoabsorption measurements by means of the equations presented here. Lastly, they provide additional information on the matrix elements needed to completely describe the interaction of the resonant state with the five continuum channels in the case of xenon.

Acknowledgments

This research was supported by the U.S. Energy Research and Development Administration under Contract no. EY-76-S-02-2892.*000. A.F.S. also received support as an Alfred P Sloan Foundation Fellow. The authors wish to thank Professor D. W. Schlitt for much help with the theoretical parameter fitting and the staff of the Wisconsin storage ring for their valuable assistance with the experiment. We are also grateful to Dr. D. L. Ederer for providing us with the data needed for Figure 1 of this paper.

References

- Dill, D. 1973 *Phys. Rev. A* **7**: 1976
- Ederer, D. L. 1971 *Phys. Rev. A* **4**: 2263
- . 1976 *Phys. Rev. A* **14**: 1936
- Fano, U. 1961 *Phys. Rev.* **124**: 1866
- . 1970 *Comm. Atom. Molec. Phys.* **2**: 30
- Fano, U., and Cooper, J. W. 1965 *Phys. Rev.* **137**: A1364
- Gardner, J. L., and Samson, J. A. R. 1973 *J. Electron Spectrosc. Rel. Phen.* **2**: 267
- . 1975 *J. Electron Spectrosc. Rel. Phen.* **6**: 53
- Samson J. A. R. 1969 *Rev. Sci. Instrum.* **40**: 1174
- Samson, J. A. R., and Cairns, R. B. 1968 *Phys. Rev.* **173**: 80
- Samson, J. A. R., and Gardner, J. L. 1973 *Phys. Rev. Lett.* **31**: 1327
- Samson, J. A. R., Gardner, J. L., and Starace, A. F. 1975 *Phys. Rev. A* **12**: 1459
- Samson, J. A. R. and Starace, A. F. 1975 *J. Phys. B: Atom. Molec. Phys.* **8**: 1806
- Starace, A. F. 1977 *Phys. Rev. A* to be published